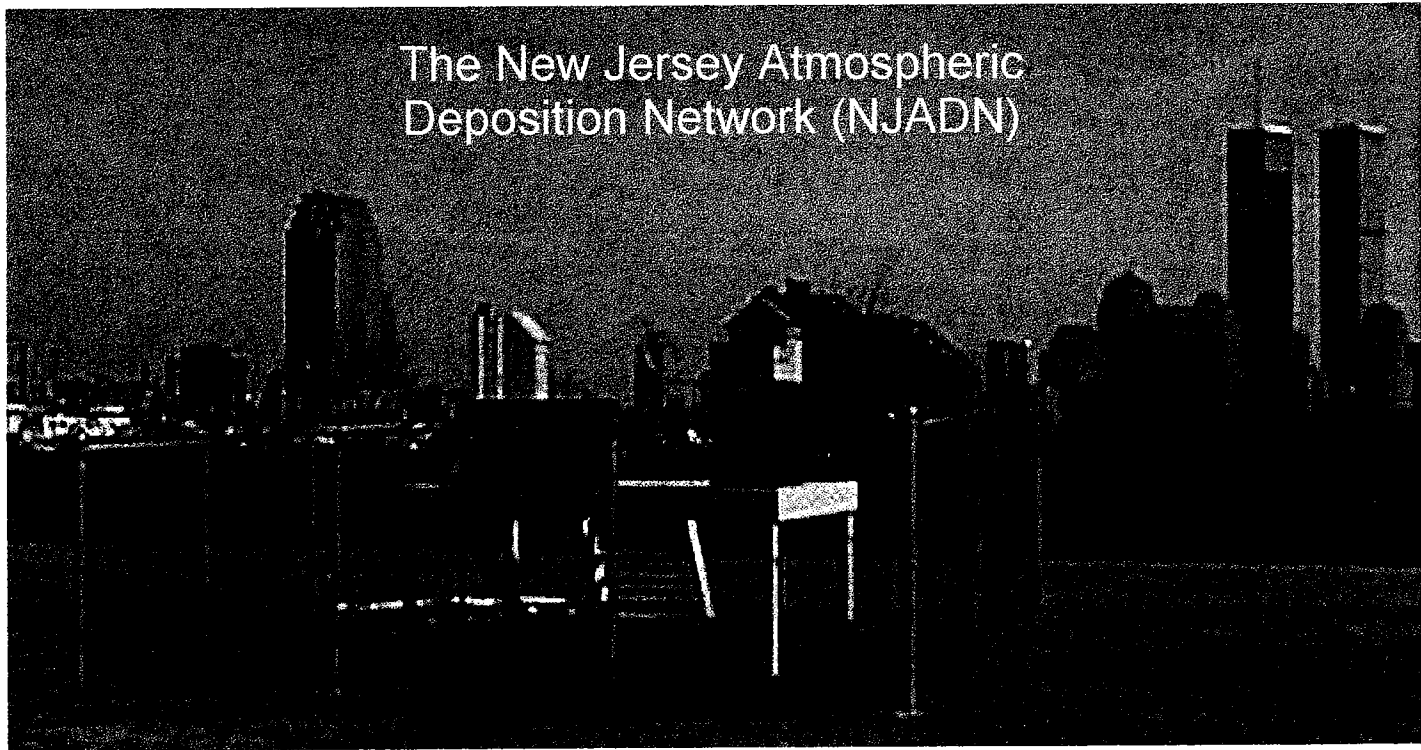


Final Report to the
Hudson River Foundation (HRF)

*Atmospheric Deposition of PCBs, PAHs, Trace Metals and Nitrogen to the
Hudson River Estuary*

Grant 001/97A

Dennis Suzskowski, Project Officer



Steven J. Eisenreich, PI

eisenreich@envsci.rutgers.edu

Department of Environmental Sciences, Rutgers University
14 College Farm Road, New Brunswick, NJ 08901

October, 2001

<u>Contributors</u>			
P.A. Brunciak*	J. Dachs	Y. Gao	C.L. Gigliotti
T.R. Glenn IV	E.D. Nelson	J. R. Reinfelder	
L.A. Totten	D.A. Van Ry	S. Yan	Y. Zhuang

o

o

o

o

o

o

o

o

o

o

o

o

Chapters

- 1. Atmospheric Deposition Of PCBs And PAHs To The NY-NJ Harbor Estuary**
- 2. Characterization Of Atmospheric Trace Elements On PM_{2.5} Particulate Matter Over The New York-New Jersey Harbor Estuary**
- 3. Atmospheric Polychlorinated Biphenyl Concentrations And Apparent Degradation In Coastal New Jersey**
- 4. Polycyclic Aromatic Hydrocarbons In The New Jersey Coastal Atmosphere**
- 5. Occurrence Of Estrogenic Nonylphenols In The Urban And Coastal Atmosphere Of The Lower Hudson River Estuary**
- 6. Atmospheric Seasonal Trends And Environmental Fate Of Alkylphenols In The Lower Hudson River Estuary**
- 7. Air-Water Exchange Of Polycyclic Aromatic Hydrocarbons In The New York-New Jersey Harbor Estuary, USA**
- 8. Dynamic Air-Water Exchange Of Polychlorinated Biphenyls In The New York-New Jersey Harbor Estuary -**
- 9. Evidence For Dynamic Air - Water Exchange Of PCDD/Fs: A Study In The Raritan Bay/Hudson River Estuary**

Appendices

- 1. PAH data**
- 2. PCB data**
- 3. Chlordane data**
- 4. Organochlorine pesticide data**
- 5. Alkylphenol data**
- 6. Quality Assurance Aspects**
- 7. Meteorological data**

* Paul Brunciak was killed in a swimming accident on November 20, 2000 in Australia within two months of the completion of his Ph.D. thesis. He assisted in the initial development of NJADN and its implementation.

o

o

o

o

o

o

o

o

o

o

o

o

o

Atmospheric Deposition of PCBs and PAHs to the NY-NJ Harbor Estuary

Lisa A. Totten¹, Cari L. Gigliotti¹, Daryl A. VanRy¹, Thomas R. Glenn IV¹, Eric D. Nelson^{1,3}, Jordi Dachs^{1,2}, and Steven J. Eisenreich^{1*}

¹Department of Environmental Sciences, Rutgers University, 14 College Farm Road,
New Brunswick, NJ 08901, USA

²Department of Environmental Chemistry, IIQAB-CSIC, Jordi Girona 18-26, Barcelona
08034

³Ecology & Environment, Inc., 11 Golden Shore Dr., Long Beach, CA 90802

* Author to whom correspondence should be addressed.

E-mail: eisenreich@envsci.rutgers.edu Phone: (732) 932-9588; Fax: (732) 932-3562

Submitted for publication to *Environmental Science and Technology*

Abstract

The first estimates of atmospheric deposition fluxes of PCBs and PAHs to the NY/NJ Hudson Estuary are presented. As part of the New Jersey Atmospheric Deposition Network, concentrations of PCBs and PAHs were measured at three sites near the estuary in air, aerosol, and precipitation at regular intervals from October, 1997 through December, 1999. Atmospheric deposition fluxes (combined gas absorption, dry particle deposition, and wet deposition) at the three sites ranged from 7.3-40 $\mu\text{g m}^{-2} \text{y}^{-1}$ for ΣPCBs and from 1400-6400 $\mu\text{g m}^{-2} \text{y}^{-1}$ for the sum of 36 individual PAHs. These depositional fluxes are at least 2-10 times those estimated for Great Waters similarly adjacent to urban areas, such as the Chesapeake Bay and Lake Michigan. Such high depositional fluxes are due to the location of the Harbor Estuary, within the urban/industrial complex of northern

New Jersey and New York City. Inputs of PCBs to the estuary from the Hudson River and from wastewater treatment plants are 8-18 times atmospheric inputs. In addition, volatilization of PCBs from the estuary exceeds atmospheric deposition by at least an order of magnitude.

Introduction

Wet deposition via rain and snow, dry deposition of fine/coarse particles, and gaseous air-water exchange are major pathways for persistent organic pollutant (POP) input to the Great Waters such as the Great Lakes and Chesapeake Bay (1, 2). Such depositional processes are especially important for aquatic systems that have large surface areas relative to watershed areas (e.g., Great Lakes; coastal seas). Many urban/industrial centers are located on or near coastal estuaries (e.g., NY-NJ Harbor Estuary (HE) and NY Bight) and the Great Lakes (e.g., Chicago, IL and southern Lake Michigan). Emissions of pollutants into the urban atmosphere are reflected in elevated local and regional pollutant concentrations and localized intense atmospheric deposition that are *not* observed in the regional signal (3, 4). The HE has been impacted by anthropogenic inputs of PCBs from wastewater discharges (5) and from historical contamination of the upper Hudson River (6). Because of its long history of contamination and its economic and environmental importance, the fate and transport of POPs in the Harbor Estuary are areas of major study (7-9). The New Jersey Atmospheric Deposition Network (NJADN) was implemented in 1997 as a research and monitoring network to assess the magnitude of atmospheric deposition of POPs, especially polychlorinated biphenyls (PCBs) and polycyclic aromatic hydrocarbons (PAHs).

Concentrations in the air, aerosol, and precipitation at three land-based sites surrounding the HE were measured from late 1997 through December 1999.

The NJADN design is based on the well-developed experience in the Great Lakes and Chesapeake Bay. The Integrated Atmospheric Deposition Network (IADN) operating in the Great Lakes (3, 4) and the Chesapeake Bay Atmospheric Deposition Study (CBADS) (10) were designed to capture the *regional* atmospheric signal, and thus sites were located in background areas away from local sources. However, many urban/industrial centers are located on or near water bodies. The southern basin of Lake Michigan and the Chesapeake Bay are two such locations subject to contamination by air pollutants such as PCBs and PAHs, Hg and trace metals (1) because of their proximity to industrialized and urbanized areas (11-21). Based on this experience in the Great Lakes and Chesapeake Bay, NJADN was designed to capture both the urban and regional signals of air pollution in the vicinity of the LHRE by locating monitoring sites in urban, suburban, and coastal environments.

In addition to receiving atmospheric inputs of POPs, water bodies may be sources of contaminants to the local and regional atmosphere representing losses to the water column. This has been demonstrated in the HE for PCBs (22) and nonylphenols (23) and chlorinated dioxins and furans (24). For this reason, the NJADN project also encompassed simultaneous measurements of POPs in the air and water of Raritan Bay (RB) and New York Harbor (NYH) in July of 1998 to estimate the dynamic air-water exchange fluxes of PAHs (22) and PCBs (25).

The objectives of this work are to estimate the atmospheric wet, dry particle and gas absorptive fluxes of PCBs and PAHs to the HE, and to provide an initial assessment of their relative importance.

Methods

Three monitoring and research sites were established at New Brunswick (NB), Sandy Hook (SH), and Liberty Science Center (LS) in Jersey City, NJ (Figure 1). In October, 1997, sample collection was initiated at NB (40.48N,74.43W), which was designed as a suburban master site located near the New Brunswick meteorological station (Rutgers Gardens) of Rutgers University. Sample collection at SH (40.46N,74.00W), began in February, 1998. SH is located south of the NY area and Manhattan and reflected the coastal marine influence on atmospheric deposition. Sample collection at LS (40.71N,74.05W) was initiated in October 1998. LS is located in the heart of the urban/industrial area across the Hudson River from New York City. Meteorological data were obtained for the LS site from the National Oceanic and Atmospheric Administration (NOAA) meteorological station located at the Newark International Airport 10 km from Jersey City. For SH, data from the NOAA station at John F. Kennedy International Airport 15 km away was used, and for NB meteorological data was obtained from the station at Rutgers University. During July 1998, simultaneous air and water samples were taken aboard the *R/V Walford* over 5 days at a site in the Raritan Bay (RB) west of Sandy Hook (40.30°N/74.05°W) from 07/05-07/98, and in New York Harbor (NYH) at the mouth of the Hudson River (39.17°N/74.02°W) west of Manhattan.

Details of sample collection, preparation, extraction and analysis can be found elsewhere (22, 24-27) and will be summarized here. Air samples (24 hours) were collected at either 9 or 12 day frequencies using a modified high volume air sampler (Tisch Environmental, Village of Cleves, OH, USA) with a calibrated airflow of $\sim 0.5 \text{ m}^3 \text{ min}^{-1}$. Quartz fiber filters (QFFs; Whatman) were used to capture the particulate phase and polyurethane foam plugs (PUFs) were used to capture the gaseous phase. QFFs were weighed before and after sampling to determine total suspended particles (TSP). Water samples during the 1998 field experiment were collected *in situ* (1.5 m depth) using an Infiltrax 100 sampling system at a flow rate of $\sim 400 \text{ mL min}^{-1}$ yielding volumes of 23-49 L. Glass fiber filters (GFFs; Whatman) with a nominal pore size of $0.7 \mu\text{m}$ were used to capture total suspended matter (TSM) and XAD-2 resin (Amberlite) was used to capture the dissolved phase. Wet-only integrating precipitation samplers were employed (Meteorological Instrument Center, MIC, Richmond Hill, Ontario, Canada) to collect integrated precipitation samples over 12-24 days in a 0.212 m^2 stainless steel funnel that drained through a glass column containing XAD-2 resin.

Analytical Procedures. Samples were injected with surrogate standards before extraction. For PCBs the surrogates were 3,5 dichlorobiphenyl (#14), 2,3,5,6 tetrachlorobiphenyl (#65), 2,3,4,4',5,6 hexachlorobiphenyl (#166), and for PAHs the surrogates were d_{10} -anthracene, d_{10} -fluoranthene, and d_{12} -benzo[e]pyrene. Samples were extracted in Soxhlet apparatus for 24 hours in petroleum ether (PUFs), dichloromethane (QFFs and GFFs), and 1:1 acetone:hexane (XAD). For XAD samples, the extracts were then liquid-liquid extracted in 60 mL Milli-Q[®] water. The aqueous fractions were back-extracted with $3 \times 50 \text{ mL}$ hexane in separatory funnels with 1 g sodium chloride. These

extracts, as well as extracts from all other types of sampling media, were then reduced in volume by rotary evaporation and subsequently concentrated via N₂ evaporation. The samples were then fractionated on a column of 3% water-deactivated alumina. The PCB fraction was eluted with hexane, concentrated under a gentle stream of nitrogen gas, and injected with internal standard containing PCB #30 (2,4,6-trichlorobiphenyl) and #204 (2,2',3,4,4',5,6,6'-biphenyl) prior to analysis by gas chromatography (GC). PCBs were analyzed on an HP 5890 gas chromatograph equipped with a ⁶³Ni electron capture detector using a 60-m 0.25 mm i.d. DB-5 (5% diphenyl-dimethyl polysiloxane) capillary column with a film thickness of 0.25 μm (27).

The PAH fraction was eluted with 2:1 dichloromethane:hexane, and injected with internal standard solution consisting of d₁₀-phenanthrene, d₁₀-pyrene, and d₁₂-benzo[a]pyrene. The PAHs were analyzed on a Hewlett Packard 6890 gas chromatograph (GC) coupled to a Hewlett Packard 5973 Mass Selective Detector (MSD) operated in selective ion monitoring (SIM) mode. The column used was a 30 m × 0.25mm i.d., J&W Scientific 122-5062 DB-5 (5% diphenyl-dimethylpolysiloxane) capillary column with a film thickness of 0.25 μm.

Quality Assurance Key quality assurance parameters are listed in Table 1. Recovery of surrogate standards, which were typically better than 90%, were used to correct individual compound concentrations for surrogate recoveries. Several PUFs were cut in half before deployment in the field in order to quantify gas phase break-through. The bottom half PUF contained on average (n=3) 13% and 12% of the total mass of PCBs and PAHs, respectively. For PCBs, the bottom half PUF contained on average less than 10%

of each individual congener (n=3), except for the trichloro PCBs, for which a maximum of 31% was found in the bottom half PUF.

Field blanks and matrix spikes were used for quality control purposes. Detection limits were determined from field blanks by taking the mean of the mass detected in all field blanks plus three times the standard deviation about the mean. The detection limit in mass units may be converted to concentration by dividing by the sample volume, which varies with each sample. Typical samples volumes are presented in Table 1. No significant differences were observed between masses of PCBs or PAHs measured in field blanks collected at the different sampling sites. Thus one detection limit was calculated which applies to all sites.

Because the concentrations of PCBs in the lab blanks were low, gas-phase PCB concentrations were corrected for surrogate recoveries but not for laboratory blanks. For PAHs, laboratory blank masses for PUFs and QFFs accounted for 0.2 to 9.3% of the total PAH (36 compounds) mass in air samples and 0.2 to 1.2% for GFFs and were subtracted from sample masses to remove the contribution of contamination occurring in the laboratory.

Framework for Deposition Calculations. Dry deposition describes the process of aerodynamic transport of a particle to the near-surface viscous sub-layer where diffusion, turbulent diffusion and gravitational settling deliver the particle to the surface. Water surfaces generally act as perfect receptors and no "bounce-off" occurs, whereas terrestrial surfaces are less efficient. Particle deposition depends on properties of the atmosphere (wind speed, humidity, stability, temperature), the water surface (waves, spray, salt content) or dry land surface, and the depositing particles (size, shape, density, reactivity,

solubility, hygroscopicity). The last may be especially important as humidity nears 100% near water surfaces permitting particles to absorb water, increase in density and size, and achieve higher deposition velocities (V_d). Zufall et al. (28) provide convincing evidence that particle deposition is dominated by large particles although atmospheric particle size distributions are dominated by particles less than 1 μm mass median diameter (mmd). Thus we selected a value for the V_d of 0.5 cm/s that reflects the disproportionate influence that large particles have on atmospheric deposition, especially in urbanized and industrialized regions (15, 29, 30). Therefore, the dry deposition flux is calculated as:

$$F_{\text{dry part}} = V_d C_{\text{part}} \quad (1)$$

where F is the flux in $\text{ng m}^{-2} \text{d}^{-1}$, and C_{part} is the seasonal average particle concentration of the POP in ng m^{-3} .

Wet deposition describes the process by which gases and particles are scavenged from the atmosphere (in cloud or below cloud) by raindrops and delivered by falling hydrometeors to the ground. Deposition of gases and particles by rain may be estimated from the fraction of the chemical in the particle and gas phase (f_{part} , f_{gas}), the total atmospheric concentration (C_T), the precipitation intensity (P), Henry's law constant as a function of temperature (H), and the particle scavenging coefficient (W_{particle} or W_{gas}):

$$F_{\text{wet, gas}} = W_{\text{gas}} f_{\text{gas}} C_T P \quad (2)$$

$$F_{\text{wet, particle}} = W_{\text{particle}} f_{\text{particle}} C_T P \quad (3)$$

where $W_{\text{gas}} = RT/H$ and W_{particle} varies from 10^2 to 10^5 (31). Due to the uncertainties inherent in the magnitude of scavenging coefficients, wet deposition was quantified by collecting rainfall at the sites, measuring the contaminant concentrations, and calculating

seasonal wet chemical deposition. Thus wet fluxes (F_{wet}) were estimated as seasonal deposition at each site as follows:

$$F_{\text{wet}} = C_{\text{VWM}} P \quad (4)$$

where C_{VWM} is the seasonal volume-weighted mean concentration of the POP in precipitation.

Calculations of absorptive gas fluxes ($F_{\text{gas,abs}}$) are described in references (18, 19, 22, 25, 32-34) and will be summarized here. The modified two-layer model used assumes that the rate of gas transfer is controlled by the compound's ability to diffuse across the water and air layer on either side of the air-water interface. The molecular diffusivity of the compound (dependent on the amount of resistance encountered in the liquid and gas films) describes the rate of transfer while the concentration gradient drives the direction of transfer. The overall flux calculation is defined by:

$$F_{\text{gas,net}} = K_{\text{OL}} \left(C_d - \frac{C_a}{H'} \right) \quad (5)$$

where $F_{\text{gas,net}}$ is the net flux ($\text{ng m}^{-2} \text{d}^{-1}$), K_{OL} (m d^{-1}) is the overall mass transfer coefficient, and $(C_d - C_a/H')$ describes the concentration gradient (ng m^{-3}); C_d (ng m^{-3}) is the dissolved phase concentration of the compound in water; C_a (ng m^{-3}) is the gas phase concentration of the compound in air which is divided by the dimensionless Henry's Law Constant, H' , $H' = H/RT$; R is the universal gas constant ($8.315 \text{ Pa m}^3 \text{ K}^{-1} \text{ mol}^{-1}$); H is the temperature and salinity-corrected Henry's Law Constant ($\text{Pa m}^3 \text{ mol}^{-1}$); and T is the temperature at the air-water interface (K). For PCBs, values for H and its temperature dependence (ΔH_H) were taken from Bamford et al. (35, 36). For PAHs, H values were estimated based on correlations between boiling point and the H values of Bamford et al.,

(37). These values are presented in ref (22). The net flux is divided into volatilization and absorption terms as follows:

$$\text{Volatilization} = K_{OL} C_d \quad (6)$$

$$\text{Absorption} = K_{OL} C_a/H' \quad (7)$$

In this study, only the absorptive gas flux was calculated from gas-phase POP concentrations measured at the land-based sites, because C_d was not available.

The overall mass transfer coefficient, K_{OL} , comprises resistances to mass transfer in both the water (k_a) and air (k_w):

$$\frac{1}{K_{OL}} = \frac{1}{k_w} + \frac{1}{k_a H'} \quad (8)$$

The mass transfer coefficients (k_a and k_w) have been empirically defined based upon experimental studies using tracer gases such as CO_2 , SF_6 , and O_2 (see refs. (38) and (39) for a review). These tracer experiments identified the importance of increasing wind speed on gas exchange rates. The air-side mass transfer coefficient for water ($k_a(H_2O)$ in $cm\ s^{-1}$) was calculated from the following relation (where u_{10} is the wind speed in $m\ s^{-1}$ at 10 meters):

$$k_a(H_2O) = 0.2u_{10} + 0.3 \quad (9)$$

This relation, recommended by Schwarzenbach *et al.* (39), has been used by many researchers in estimating air-water exchange fluxes (18, 19, 32-34). The quadratic relationship of Wanninkhoff was used to predict k_w in this study (38):

$$k_w(CO_2) = 0.45u_{10}^{1.64} \quad (10)$$

Differences in molecular diffusivity between these gases and PCBs and PAHs were then used to estimate k_a and k_w for PCBs and PAHs. Unlike dry particle and wet depositional

fluxes, calculation of $F_{\text{gas,abs}}$ requires knowledge of air and water temperature and wind speed. For this reason, $F_{\text{gas,abs}}$ was calculated separately for each day of sample collection and the results averaged to yield a seasonal estimate of $F_{\text{gas,abs}}$.

Results and Discussion

Air Temperatures, Wind Speed, and Precipitation

Calculation of dry particle deposition, wet deposition and gas absorptive fluxes of target organic chemicals to the NY-NJ Harbor Estuary requires knowledge of the air temperatures and wind speeds at the three sites surrounding the HE (NB, SH, LS), and the mean surface skin temperature of the water body. The mean daily air temperatures ranged from approximately 0°C in the winter to 22-25 °C in the summer. Specific meteorological data for each site are given the Table 1 of Supporting Information. The mean daily surface skin temperature in the open estuary, determined by remote sensing in the IR band, follows the air temperature closely as expected due to coupling of the air and water (40). For this reason, air temperatures were used to calculate gas absorption. The mean daily wind speeds at the SH and LS sites on the estuary were higher than at the land-locked NB site on all sampling days, yielding conservative estimates of exchange at the latter. Typical daily mean wind speeds at NB were generally ~ 2-4 m s⁻¹ whereas wind speeds at the other sites ranged from 2 to as much as 12 m s⁻¹ depending on storm activity, season, and sea breezes.

Precipitation intensity or volume was summed over the four seasons of winter (Dec-Feb), spring (March-May), summer (June-August), and fall (September-November) and are given in Table 2 of Supporting Information. The volume of collected precipitation per sampling interval varied from 0.04 to 67 L. The mean annual

precipitation (30-year average) for the HE is $\sim 1.1 \text{ m y}^{-1}$ (<http://climate.rutgers.edu/stateclim/norms/precip.html>). Precipitation intensity over the study period ranged from 0.9 m y^{-1} at NB to 1.68 m y^{-1} at the LS, the latter being mostly due to locally intense summer rains.

Polychlorinated Biphenyls (PCBs)

Tables 2-4 present seasonally-averaged PCB concentrations in the gas, particle, and precipitation phases at each of the three sites. Before presenting the estimates of atmospheric deposition derived from these data, trends in atmospheric concentrations of PCBs will be briefly examined.

Gaseous concentrations of ΣPCB at NB varied from 39 to $2,300 \text{ pg m}^{-3}$ and from 80 to $1,000 \text{ pg m}^{-3}$ at SH. These ranges are similar to those reported by Brunciak et al. (27) for the same sites over a shorter reporting period (ending April 1999, versus December 1999 for this report). The additional eight months of data included in this report allow a more comprehensive assessment of the dynamics of atmospheric PCB concentrations at LS, where gas-phase concentrations ranged from 96 to $3,500 \text{ pg m}^{-3}$. Gas-phase concentrations were lower at SH than at NB on 29 of 37 sampling days. Gas-phase concentrations were higher at LS than at NB on all sampling days. These concentrations are higher than those measured by other researchers at rural sites such in Hazelrigg, UK (41), in the Great Lakes at IADN; refs (3, 42, 43)), and those measured over the water of the Chesapeake Bay (19, 44). (See Brunciak et al. (27) for a summary). Gas-phase ΣPCB concentrations measured over water during July 1998 were highest at LS, lower over Raritan Bay and New York Harbor, and lowest at coastal SH (25). Although the temporal trends of total concentrations were different at the three sites,

Brunciak et al. (27) previously noted that the PCB congener profiles were similar, implicating a dominant emission type and/or process. The larger data set reported herein further supports this conclusion.

At NB, SH, and LS, temperature explained 35%, 56%, and 54% of the total variability in gas-phase PCB concentrations, respectively. The lesser importance of temperature on PCB concentrations at NB in this study is in contrast to the conclusion of Brunciak et al. (27) that temperature explained >50% of the total variability in gas-phase PCB concentrations at all sites (27). This difference is largely due to the inclusion of 4 samples taken during the winter of 1998-1999 which displayed the lowest concentrations of PCBs measured at that site. These concentrations were significantly lower than would be predicted from the $\ln P$ vs. $1/T$ relationship. At each site, Brunciak et al. (27) used the following relation to investigate the influence of wind speed (u in m s^{-1}) and direction (wd in degrees) on gas-phase PCB concentrations (C_{gas}):

$$\ln C_{gas} = a_0 + a_1 / T + a_2 \ln(1/u) + a_3 \sin(wd) + a_4 \cos(wd) \quad (11)$$

Where a_x values are fitting parameters. This multiple linear regression reveals that T alone is a significant predictor of gas-phase PCB concentrations at NB, LS, and SH at the 95% confidence level. This is in contrast to the previous reports of Brunciak et al. (27), who noted that atmospheric PCB concentrations at NB increased when winds blew from an east-northeast vector, while increased wind speeds led to a 20-40% dilution.

Particle phase PCBs represent from 0.6 to 45% of the total concentration (gas + particle), with higher percentages occurring during colder sampling periods due to the decrease in vapor pressure of PCB congeners at lower temperatures increasing sorption onto airborne particles. As with gas phase concentrations, particulate concentrations of

Σ PCBs were highest at LS and lowest at SH on the majority of sampling days. Particulate concentrations ranged from 7.1 to 164 pg m^{-3} at LS, from 4.2 to 142 pg m^{-3} at NB, and from 0.66 to 44 pg m^{-3} at SH.

Concentrations of Σ PCBs in precipitation varied from 0.27 to 106 ng L^{-1} at the three sites. Highest concentrations were measured in the smallest (by volume) precipitation samples, as expected due to efficient scavenging of gases and particles at the onset of the precipitation event. Thus concentrations presented in Tables 2-4 are seasonal volume-weighted means. These range from 9.8 to 0.46 ng L^{-1} with highest concentrations typically occurring in winter.

Tables 2-4 also present a summary of the dry particle deposition, wet deposition and gas absorption of Σ PCBs and PCB homologues seasonally at LSC, NB and SH ($\text{ng m}^{-2} \text{d}^{-1}$). These are the first comprehensive estimates of atmospheric PCB deposition to the NY-NJ Harbor Estuary and the Lower Hudson River Estuary. The gaseous PCB concentrations at NB were included in the calculation of gas absorption into the HE because it is close to the Raritan River and is thus part of the estuary. However, lower wind speeds at NB when compared against open water sites result in lower apparent PCB gas absorptive fluxes at NB. All three depositional processes combined result in fluxes of 40, 7.3, and 15 $\text{ug m}^{-2} \text{y}^{-1}$ at LS, NB, and SH, respectively. Gas absorption is by far the largest component of atmospheric deposition at LS and SH, but is similar to particle deposition at NB. Dry particle and wet deposition fluxes of PCBs are highest at LS and lowest at SH. Gas absorption fluxes, however, are lowest at NB, despite higher gas-phase PCB concentrations, due to lower winds speeds. No clear seasonal trends in deposition are evident. This lack of seasonality arises in part because low T during the

winter has two effects which partially negate each other: Henry's law constants decrease with decreasing T (35, 36), resulting in an increased tendency toward gas absorption, and gas-phase PCB concentrations are also lower during the cold winter months, with lower concentrations available for gas absorption.

The estimated fluxes of Σ PCBs to the HE may be compared with those estimated for other aquatic systems. The sum of wet and dry particle deposition of Σ PCBs to the Chesapeake Bay estimated from CBADS data (1) and for the Great Lakes from IADN data (3, 4) are 1.8-3.3 and 1.0-2.5 $\mu\text{g m}^{-2} \text{y}^{-1}$, respectively. Comparing only wet and dry particle deposition amongst the systems, the HE is loaded at a rate of approximately 2 to 10 times these aquatic systems. At LS and SH, gaseous deposition of Σ PCBs dominates the overall depositional flux. Lower air concentrations of Σ PCBs in the Great Lakes and Chesapeake Bay areas suggest that gas deposition fluxes to these waters are not likely to exceed those to the HE (3, 11, 19, 42-44). Thus it is likely that the overall atmospheric deposition fluxes of PCBs to the HE are at least 2 – 10 times those experienced in the Great Lakes and Chesapeake Bay.

Compared with other inputs of PCBs to the HE, atmospheric deposition is small (Figure 2). Twenty-six water pollution control plants discharge 88 kg of PCBs per year to the HE (5). Farley et al. (7) estimate that in 1997 at least 180 kg y^{-1} was advected into the estuary from the Hudson River. Assuming that the plume of atmospheric contamination extends throughout the Raritan Bay and the New York/New Jersey Harbor area, the current estimates of atmospheric deposition result in about 10 kg y^{-1} of Σ PCBs being deposited into the estuary.

The high concentrations of PCBs in the water column of the HE coming from upstream flow in the Hudson River, other tributary inputs, and discharges from waste water treatment facilities contribute to a large volatilization flux (25). Totten et al. (25) report the absorptive, volatilization and net fluxes of PCBs from the HE for July 1998 based on simultaneously measured air and water concentrations of PCBs in Raritan Bay and New York Harbor. In Raritan Bay, the depositional flux (Σ PCBs) averaged $-25 \text{ ng m}^{-2} \text{ d}^{-1}$, similar to the gas deposition fluxes estimated for the LS and SH sites. However, the volatilization flux averaged $+420 \text{ ng m}^{-2} \text{ d}^{-1}$, swamping the depositional flux. Tri- and tetra-chlorinated PCBs constitute more than 85% of the volatilization signal. Congeners containing 6-9 chlorines were near equilibrium with respect to air-water exchange. It is difficult to extrapolate these results, based on a limited number of samples in one season, to obtain a larger picture of the cycling of PCBs in the HE. However, net air-water exchange fluxes of PCBs are expected to remain positive throughout the year due to the large water-air fugacity gradient and relatively constant seasonal water concentrations (25). Volatilization of PCBs from the estuary is likely to remain greater than atmospheric deposition (wet, dry particle, and gaseous deposition) throughout the year, suggesting that the estuary acts as a net source of PCBs to the local atmosphere, consistent with the conclusions reached by Brunciak (45).

Polycyclic Aromatic Hydrocarbons (PAHs)

Atmospheric concentrations were measured for 36 individual PAHs with molecular weights ranging from 166 (fluorene) to 300 g mol^{-1} (coronene). The seasonal average concentrations for the 36 PAH compounds in the gas and particle phases and precipitation are presented in Tables 2-4. Total gas phase PAHs, defined as the sum of

the gas phase concentrations of the 36 measured PAHs, at the suburban NB site ranged from 3.2 to 84 ng m⁻³. Total gas phase PAHs were higher at the urban/industrial LS site where concentrations ranged from 7.5 to 92 ng m⁻³. Concentrations were lowest at the coastal SH site (ranging from 0.45 to 52 ng m⁻³) due to its location away from the immediate impact of heavy traffic arteries, industry, and urbanization as seen at the other two sites. The majority of the discussion following will focus on three individual compounds (phenanthrene, pyrene, and benzo[a]pyrene) that span the wide range of physical and chemical properties and atmospheric speciation in the compound class PAH.

Concentrations of gas phase phenanthrene (MW = 178 g mol⁻¹) ranged from 0.49 to 21 ng m⁻³ at NB, from 0.14 to 14 ng m⁻³ at SH, and from 3.4 to 34 ng m⁻³ at LS. Gas phase pyrene (MW = 202 g mol⁻¹) concentrations ranged from 0.0048 to 2.3 ng m⁻³ at NB, 0.0080 to 2.3 ng m⁻³ at the SH, and from 0.16 to 4.3 ng m⁻³ at LS. Gas phase benzo[a]pyrene (MW = 252 g mol⁻¹) concentrations were below detection limits in 78% of samples at NB (n=135), 90% at SH (n=73), and 73% at LS (n=56), with maximum concentrations of 0.13 ng m⁻³ at NB, 0.017 ng m⁻³ at SH, and 0.014 ng m⁻³ at LS. In general, gas phase PAH concentrations were highest in the urban/industrial area (LS) and lower at NB and SH. Gas phase PAH concentrations at LS were higher than those at NB on 50 of 52 days, and higher than those at SH on 32 of 35 days. The ranges reported for NB and SH are similar to those reported by Gigliotti et al. (26) for the same sites over a shorter sampling period (October 1997 – December 1998).

Gas phase PAH concentrations measured at LS, while higher than those measured at SH and NB, are nevertheless lower than those measured in urban/industrial Chicago, IL as part of AEOLUS (11) but similar in magnitude to those measured in

urban/industrial Baltimore, MD (20). Concentrations measured at the coastal SH site are as much as an order of magnitude higher than concentrations measured as part of the IADN at remote sites in the Great Lakes region (3), suggesting that coastal SH is impacted by significant PAH emissions from multiple directions. PAH concentrations measured over-water in the NY-NJ Harbor Estuary during a July 1998 intensive sampling campaign were found to be lower than those measured over-water in Lake Michigan (11) and the Chesapeake Bay (19).

An investigation of the importance of meteorological parameters including wind speed, wind direction, and T on gas phase PAH concentrations was performed using equation 11. At NB, T is a significant ($p < 0.05$) predictor of gas-phase concentrations for phenanthrene ($R^2 = 0.22$), fluoranthene ($R^2 = 0.25$), and the methylated phenanthrenes ($R^2 = 0.12$), but is not significantly correlated with concentrations of any other PAHs. At SH, no significant correlations were observed between gas-phase PAH concentrations and T. The lack of correlation between T and PAH concentration at these two sites suggests that, in contrast to the PCBs, air-surface exchange processes are less important in controlling PAH concentrations, a conclusion reached by other researchers (46). Concentrations of all PAH compounds were found to be independent of wind direction and wind speed at NB and SH suggesting that the region surrounding the NY-NJ Harbor Estuary is influenced by PAH emissions from all directions.

The situation at LS is more complicated. If the 4 samples from winter 1998-1999 discussed in the PCB section are excluded from the analysis via equation 11, concentrations of 3 of the 36 PAHs show significant correlations ($p < 0.05$) with T at LS: phenanthrene ($R^2 = 0.26$), fluoranthene ($R^2 = 0.37$) and pyrene ($R^2 = 0.26$). No

significant correlation between any PAH concentrations and wind speed or wind direction was observed at LS when these samples are excluded. However, in these 4 samples, the wind was from a N-NW vector and the mean concentration for each of the 36 PAHs was significantly lower (t-test – 95% confidence level) than the mean for the rest of samples taken at LS. Because of the coupling of low PAH concentrations with low T and N-NW winds in these 4 samples, their inclusion improves the overall correlation, such that both T and wind direction become significant predictors of concentration for 5 PAHs (phenanthrene $R^2 = 0.40$; anthracene $R^2 = 0.38$; pyrene $R^2 = 0.50$; fluoranthene $R^2 = 0.54$; methylated phenanthrenes $R^2 = 0.37$), and wind direction alone becomes significant for benzo[a]pyrene ($R^2 = 0.21$).

Concentrations of total particle phase PAHs (36 compounds) ranged from 0.38 to 16 ng m^{-3} , 0.14 to 5.7 ng m^{-3} , and 0.24 to 32 ng m^{-3} at NB, SH, and LS, respectively. Particle phase phenanthrene concentrations ranged from below detection limits to 1.1 ng m^{-3} at NB, from 0.0065 to 1.1 ng m^{-3} at SH, and from 0.0022 to 1.2 ng m^{-3} at LS. Pyrene concentrations ranged from below detection limits to 1.4 ng m^{-3} at NB, from below detection limits to 0.39 ng m^{-3} at SH, and from 0.018 to 3.8 ng m^{-3} at LS. Benzo[a]pyrene ranged from below detection limits to 0.73 ng m^{-3} at NB, from below detection limits to 0.21 ng m^{-3} at SH, and from 0.0017 to 1.3 ng m^{-3} at LS. As with gas-phase PAHs, concentrations of total particle phase PAHs ($n = 36$) are higher at LS than NB on 42 of 52 days and higher than at SH on 29 of 32 days. The higher concentrations of PAHs measured at LS are consistent with its proximity to urban/industrial areas.

In precipitation, total PAH concentrations ($n = 36$) ranged from 38 to 1640 ng L^{-1} , from 22 to 3170 ng L^{-1} and from 31 to 1330 ng L^{-1} at NB, SH, and LS, respectively.

Phenanthrene concentrations ranged from 3.9 to 148 ng L⁻¹ at NB, from 2 to 313 ng L⁻¹ at SH, and from 5.5 to 133 ng L⁻¹ at LS. Pyrene concentrations ranged from 0.14 to 140 ng L⁻¹ at NB, 0.49 to 319 ng L⁻¹ at SH, and 1.4 to 111 ng L⁻¹ at LS. Benzo[a]pyrene concentrations ranged from below detection limits to 51 ng L⁻¹ at NB, 0.53 to 161 ng L⁻¹ at SH, and 1.2 to 61 ng L⁻¹ at LS. As with PCBs, the highest PAH concentrations are associated with the smallest volumes of precipitation. Volume weighted mean concentrations (Tables 2-4) were thus used in the calculation of seasonal wet depositional fluxes.

Atmospheric PAH concentrations exhibit a distinct seasonality such that gas and particle phase concentrations are highest in the winter and lowest in the summer. This trend arises from increased fuel usage in winter leading to enhanced emission of PAHs (47-49).

A comparison of the atmospheric depositional fluxes (dry particle deposition, wet deposition, and gas absorption) at all three sites is presented in Tables 2-4. Seasonal average total atmospheric depositional fluxes (dry particle + wet + gas absorption) of total PAHs (36 compounds) range from 2.1 µg m⁻² d⁻¹ at NB in summer to 22 µg m⁻² d⁻¹ at LS in spring. Gas absorption dominates the total flux of lower molecular weight compounds (166 to 234 g mol⁻¹) and is less important as MW increases.

Unlike PCBs, PAHs display distinct seasonal trends in dry particle depositional fluxes that are highest in winter and lowest in summer at all three sites, consistent with the trend in absolute concentrations. At both NB and LS, the largest wet depositional fluxes occur in winter. At SH, however, the largest wet fluxes occur in the spring. The